Single Anchor Localization by Combining UWB Angle-of-Arrival and Two-Way-Ranging: an Experimental Evaluation of the DW3000.

Ben Van Herbruggen, Stijn Luchie, Ruben Wilssens and Eli De Poorter
INTEC-IDLab, Ghent University-imec, Ghent, Belgium
ben.vanherbruggen@ugent.be

***Abstract*—Ultra-wideband (UWB) provides cm-level accuracy even in large-scale industrial settings. However, UWB deployment is hindered by the need for fixed infrastructure nodes requiring power and cabling. To address these challenges, a single anchor node can provide position estimates by leveraging both time and phase information, thereby simultaneously estimating both the distance and 2D angle-of-arrival (AoA) of incoming UWB packets. At this moment no studies evaluate the accuracy of commercial single-anchor node deployments. Therefore, in this study, we empirically validate a single-anchor localization setup utilizing the IEEE802.15.4z compliant DW3000 transceiver. Our results indicate that estimating the angle based on the channel impulse response (CIR) yields greater accuracy compared to values reported by the transceiver. When integrating angle and distance information, a single anchor achieves a mean accuracy of up to 43.3 cm over a 50 m^2 area. Furthermore, we observe that increasing the number of anchors improves the accuracy of the localization system. Interestingly, the inclusion of additional angular information when 3 or more anchor nodes are present does not significantly enhance system performance compared to traditional TWR positioning algorithms.**

***Index Terms*—ultra-wideband, UWB, angle-of-arrival, AoA, two-way-ranging, TWR, single-anchor localization**

I. Introduction

The increasing demand for accurate location-based services has fueled the exploration of novel indoor localization solutions. Among the possible technologies for indoor localization systems, ultra-wideband (UWB) technology is a promising candidate with high resilience against multipath effects and low transmission power [1]. The utilization of the wide bandwidth of signals allows for high-resolution timestamping and therefore precise localization.

Traditional indoor localization systems consist of fixed infrastructure nodes and mobile tags to localize. To obtain a good localization performance, the mobile tag needs good coverage over the whole deployment. In these UWB systems three localization techniques are commonly used: two-way-ranging (TWR), time-difference-of-arrival (TDoA), and angle-of-arrival (AoA) [2], [3]. TWR is the most used localization technique and estimates the distance between the tag and anchor. TDoA localizes the tag based on the difference in arrival time of signals at the anchor nodes, but this approach requires that the anchor nodes are nearly perfectly synchronized. The last method, AoA, is less frequently used due to the hardware requirements (multiple receiving antennas). Recently, the commercialization of UWB has sped up with the introduction of novel transceivers and the standardization efforts [4]. The new generation of UWB transceivers has multiple RF ports to support AoA.

In this paper, we delve into reducing anchor nodes towards less dense anchor deployments, even with only a single anchor node. The single anchor localization is possible due to the recently launched DW3000 transceiver and its AoA capabilities. With the combination of angle and distance information, the tag can be localized without ambiguity. In addition, no synchronization between the anchor nodes is required. The reduction of the number of anchor nodes in UWB deployments results in lower deployment costs and simplifies the system complexity. By relying on a single anchor, this method uses the unique capabilities of UWB technology to achieve high-precision location estimates in diverse and challenging environments. This paper aims to provide an experimental overview of the capabilities of single anchor localization compared to traditional UWB localization systems. The paper experimentally investigates various aspects, including evaluating range and angle results, localization algorithms, and practical considerations such as the number of anchor nodes.

The main contributions of this paper are:

- The AoA and TWR accuracy is evaluated on using the recent commercial-off-the-shelf (COTS) DW3000 IEEE802.15.4z compliant radio transceiver.
- The accuracy of different AoA estimation techniques (phase-difference-of-arrival (PDoA) and channel impulse response (CIR) based) are compared.
- The localization accuracy of using either TWR, AoA, or a combination of both is evaluated for varying numbers of anchor nodes.
- The accuracy of the system for track-and-tracing use cases, which allow exploiting temporal redundancy through the use of e.g. Kalman filtering and averaging, is evaluated.

Together, these contributions give clear insights into the trade-offs and expected accuracies of different single-anchor node configurations and setups.

This research is partially funded by Research Foundation - Flanders (FWO) PESSO project under grant number: G018522N.

979-8-3503-8078-1/24/$31.00

The remainder of this paper is structured as follows: Section II discusses state of the art (SOTA) research on single anchor localization. In Section III, the algorithms for determining the angle and distances are explained. The data collection is described in Section IV which are followed by the localization algorithms that were used for the evaluation in Section V. The results are presented in Section VI. In Section VII, we discuss potential future research directions enabled by this paper. This paper is concluded in Section VIII.

II. Related work

The DW1000 transceiver is widespread in academic literature with a plethora of applications. With the introduction of its successor in 2020, the DW3000, Qorvo added a second radio frequency (RF) input to the transceiver enabling switching between two different antennas in the same UWB packet and therefore making AoA possible. A beta kit, the DWM1002, specifically targetting AoA based on the DW1000 has been released. The paper [5] discusses the theoretical background on PDoA and experimental results. Botler et al [6] used this beta kit to train machine learning (ML) models. They tested different regressors and concluded that the random forest regression was the best fit for their experimental data with a mean absolute error (MAE) of 8°.

Tiemann et al [7] presented CELIDON, a hardware platform with three DW1000 transceivers and the possibility to estimate the AoA with PDoA. The hardware can be integrated into firefighter's equipment, enabling ad-hoc localization. In laboratory conditions, they achieved a direction estimation accuracy of 20° and a position finding accuracy of 30 cm. Naseri et al [8], followed a similar approach with four DW1000 transceivers and applied PDoA, multiple signal classification (MUSIC), and ML algorithms to estimate the angles. The field of view with the PDoA and MUSIC algorithms is limited to 90°. All the previous papers require multiple transceivers in one node while our approach works with a single transceiver.

AoA was already included in the evaluation of the Ubisense real time location system (RTLS) by Ruiz et al [9]. This paper discussed three different UWB systems from different vendors for their accuracy. The Decawave system was the most accurate, but only Ubisense could add angle information to the localization, however with limited accuracy. The research on AoA with the newer DW3000 transceiver is more limited. Similar to AoA, angle-of-departure (AoD) enables new use cases. This concept is introduced by Han et al [10]. Customized hardware has been developed to shift the phase of the packet components and transmit at a certain angle.

Other single anchor localization solutions exploit room information to use reflections for localization [11]–[13]. In contrast to these solutions, our single anchor localization approach does not require room information.

III. Background information TWR and AoA

To establish a solid foundation for our exploration of UWB single anchor localization, this paper begins by delving into the background information surrounding two fundamental localization techniques: two-way-ranging (TWR) and angle-of-arrival (AoA). The packets transmitted by the UWB devices are compliant with the IEEE802.15.4z standard, and include an scrambled timestamp sequence (STS) part. The STS is transmitted immediately after the preamble and is required for determining the incident angle. The packet structure is given in Fig. 1. The packet starts with the synchronization header (SHR), which contains the preamble and the start-of-frame delimeter (SFD). The timestamping at the transmitter and receiver is done at the SFD. After this SHR, the STS is transmitted which is added to the packet structure by the standard mainly for security but also provides to extra CIRs that can be used for AoA. In our paper, the STS is transmitted immediately after the SHR but the standard specifies multiple packet structures where the position of the STS changes [4]. The two last parts of the packet are the PHY header (PHR) and the PHY payload.

Fig. 1: Packet structure used for the single anchor localization. The STS adds both security and AoA possibilities. The payload is required for communicating timestamps between the initiator and responder.

A. TWR

TWR is a localization technique that measures the distance between two UWB devices. This procedure involves measuring the time taken for a signal to travel between the anchor and the tag. This time-of-flight (ToF) is used together with the speed of light c to retrieve the distance with Equation 1.

$$d = ToF \times c \tag{1}$$

Different variants exist for TWR with sending two, three, or four packets over the UWB connection between tag and anchor. The two packet schemes (single sided two-way-ranging (SS-TWR)) handle clock offsets but are sensitive to the drift of both clocks. To overcome this, a third packet is introduced in double sided two-way-ranging (DS-TWR) which incorporates clock synchronization between sender and receiver. In this three-packet scheme, the initiator, in our case the tag, transmits the $poll$ message. All anchor nodes listen to this message but only the anchor targeted by the tag will respond with a $reply$ message. After receiving this $reply$ message, the tag will send a $final$ message including its three timestamps $t1$, $t4$, and $t5$ in the PHY payload (see Fig. 1). Based on these three timestamps and the three timestamps measured at the anchor itself, it is possible to calculate the ToF with Equation 2. An optional fourth packet can be transmitted from the responder to the initiator to inform the initiator of the approximated distance. After the calculation of the distance between the tag and an anchor, the tag immediately starts the same message scheme with the next anchor. Distances to multiple anchors can be combined with trilateration into a single position. The message protocol is shown in Fig. 2.

$$ToF = \frac{(t_4 - t_1) \times (t_6 - t_3) - (t_5 - t_4) \times (t_3 - t_2)}{((t_4 - t_1) + (t_6 - t_3) + (t_5 - t_4) + (t_3 - t_2))} \quad (2)$$

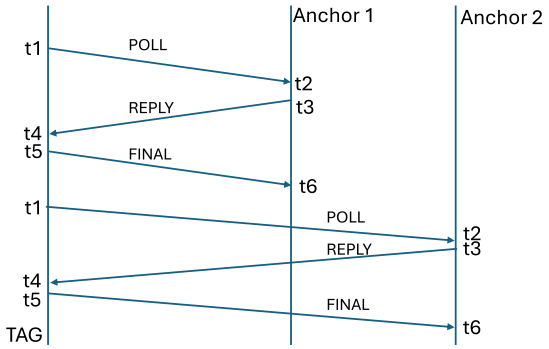

Fig. 2: A three-packet scheme is followed for the TWR. The tag initiates the scheme with a POLL message. The selected anchor responds with a REPLY message after which a FINAL message is sent to the anchor.

B. AoA

The main idea behind AoA UWB is figuring out the direction from which a signal is coming to the receiver. This is achieved through signal processing algorithms that analyze phase differences between signals received by different antennas. The DW3000 transceiver has two RF ports. During the reception of the STS, the transceiver switches the antenna ports. From both antennas the STS will result in a CIR and the difference in phase at both antennas will be characteristic of the incident angle. The angle is determined based on the phase of the internal clock at the reception of both STS parts and calculated with Equation 3.

$$\theta = arcsin(\frac{(\phi_1 - \phi_2) \times \lambda}{2\pi \times d}) \quad (3)$$

with d the separation between the antennas (1.82 cm) and λ the wavelength. The separation depends on the wavelength of the signal. The wavelength depends on the signal frequency (f) and the speed of light (c) (see Equation 4).

$$\lambda = \frac{c}{f} \approx 4.61cm \quad (4)$$

IV. Data collection

This section outlines the data collection: it begins with a discussion of the measurement setup used for experimental validation. By transparently presenting our experimental methodology, readers gain insights into the practical considerations that support our investigation, laying the groundwork for a thorough evaluation of the UWB single anchor localization system.

The experiments were organized in the IIoT lab at Ghent University which represents an industrial warehouse environment. The lab is divided into two main parts: an open space area and an area with metal racks. For this first evaluation, the open space area is used to limit the amount of NLOS. However, the metal objects are near the measurement area and still reflect UWB signals. The lab is equipped with a mm-accurate motion capturing (MOCAP) system which enables analysis of the single anchor localization with both accurate ground truth and repeatable trajectories with a mobile robot. The used UWB hardware consists of 4 DW3000-based nodes. The DW3000 transceiver is controlled from a Nordic nrF52840 development kit board with a Zephyr stack. The mobile robot executes the trajectory of 113 m at 0.3 m/s (see Fig. 3) while the tag is ranging with all four anchors. All UWB anchors are connected to a dedicated high-throughput cabled network to collect data from all anchor nodes with a high update rate. The UWB operates at channel 5 with 512 preamble symbols, 512 STS symbols, and 64 MHz PRF resulting in a short but stable link. In total about 11 607 successful ranges were collected in the dataset. For the evaluation of results, no outliers are removed from the dataset but a time correction has been applied to one of the anchor nodes due to 0.5s latency in the collection of the data from the anchor nodes. This latency is only dependent on the data collection and doesn't influence conclusions from the paper.

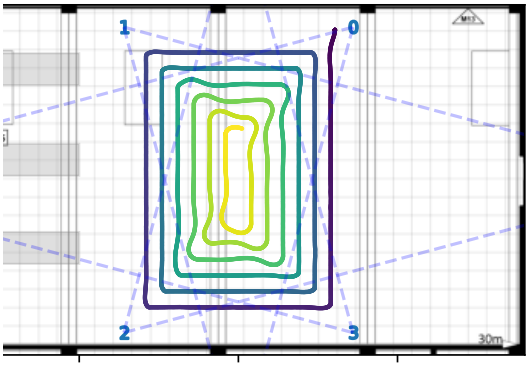

Fig. 3: Trajectory in the lab covering the open space for the data collection. Four anchors and one tag are used. The trajectory is inside the 45°field of view of most anchors.

To facilitate both localization techniques with a high update rate, a time division multiple access (TDMA) medium access control (MAC) layer is used. The tag follows a fixed protocol where every anchor receives one slot for the TWR message exchange. In this slot, two packets are transmitted from the tag and one in between from the anchor node to estimate the distance with DS-TWR. The third packet of this message exchange is also used to determine the anchor's incident angle.

V. Localization

The individual ranges and angles that are measured need to be combined into positions. In this section, we will briefly discuss frequently used trilateration and triangulation algorithms to approximate the mobile tags position. The localization algorithms are similar for the three localization techniques.

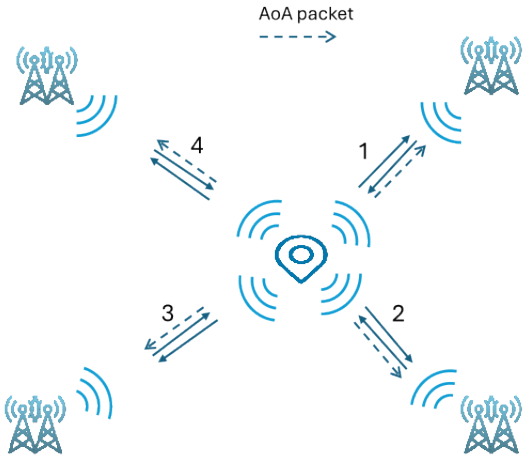

Fig. 4: The tag executes three packets with the four anchors to combine AoA and TWR.

A. TWR localization

Least squares: In a 2D positioning system, each range creates a circle indicating potential tag locations. Ideally, these circles result in one intersection. However, in realistic conditions, noise is introduced in the hardware and during propagation which eventually results in the need for an optimization algorithm. The least squares algorithm resolves this, finding the point closest to all circles as the tag's likely position. The cost used for the optimization problem is the sum of all distances to this approximated point, see equation 5, where $\vec{P}_{tag}$ is defined as the estimated position of the tag, $\vec{P}_{anchor_i}$ is defined as the position of anchor i and $\vec{d}_i$ is a vector representing the estimated distance and direction to the tag concerning anchor i. For this least-squares approach, the localization is done based on the last four correct ranges but no previous positioning information is taken into account.

$$cost = \sum_{i=0}^{N} |||\vec{P}_{anchor_i} - \vec{P}_{tag}|| - ||\vec{d}_i||| \tag{5}$$

Kalman filter: A second approach can be used: the localization server combines the distances measured with TWR and the anchor coordinates to a position estimate using a Kalman filter [14]. A Kalman filter smooths the localization points by estimating where an object is and how fast it's moving in both directions. The state vector of this Kalman filter consists of position (x,y) and velocity (v_x,v_y). It works in two steps: 1) predicting the next state based on the previous one and uncertainties on ranging information ($\sigma_w = 25$ cm) and on the movement information ($\sigma_v = 10$ cm/s), and 2) updating with measurements from the UWB links. The Kalman gain, calculated with the difference between the prediction and measurement, represents measurement certainty. This, in turn, adjusts the state. Every new UWB measurement triggers both steps, updating the filter's state. The Kalman filter's only input is the UWB measurement, and it takes no input from any other sensor.

B. AoA localization

Least squares: The position of the mobile tag is determined by the intersection of the two half-lines corresponding with the angles starting at the fixed anchor nodes. This optimization problem is solved with a least-squares approach. The estimated point is the point with the lowest cost where the cost is defined as the distance to all half lines from the anchor nodes, see equation 6.

$$cost = \sum_{i=0}^{N} \frac{(\vec{d}_i - \vec{P}_{anchor_i}) \times (\vec{P}_{tag} - \vec{P}_{anchor_i})}{|\vec{d}_i - \vec{P}_{anchor_i}|} \tag{6}$$

Kalman filter: A second variant of the Kalman filter is used for estimating the positions with angle information included. As the angle information includes non-linearity and the distribution of the measurement noise, not Gaussian, the Kalman filter will take the positions estimated with least-squares (LS) as input and smooth the trajectory. The state vector of this Kalman filter is the same as in the other variant but the uncertainty is tuned differently ($\sigma_v = 100$). More advanced version of a Kalman filter, such as an extended Kalman filter (EKF) or unscented Kalman filter (UKF) or particle filter can be used to integrate these non-linearity effects in the position estimation.

C. AoA and TWR localization

Least squares: The position of the mobile tag can also be determined by combining the methods of TWR & AoA localization. This can be achieved by having the cost functions which the Least-Squares solver will optimize be the sum of both the TWR (eq. 5) & AoA (eq. 6) cost functions. The optimization of this new cost function will result in the estimation of the global position of the mobile tag.

Kalman filter: The same Kalman filter as with AoA is used which takes positions as input.

VI. Results

In this section, we will evaluate the localization's performance based on the collected experimental data. We will first evaluate the ranging performance of the DW3000 modules. Secondly, the estimation of the AoA is discussed in detail. Based on these results the localization performance of TWR, AoA, and both techniques combined is evaluated.

A. Ranging accuracy

The TWR ranging performance is evaluated for all four anchor nodes. The MAE of the ranging error, the difference between the measured distance and the true distance, is 10.1, 6.1, 7.5, and 6.8 cm for the four separate anchors. For all anchors, the ranging is on average 7.6 cm accurate over an area of 50 m^2 for varying incident angles. These reported ranging accuracy is well within the expected results from other literature. The cumulative distribution function (cdf) curve for the ranging error is given in Fig. 5.

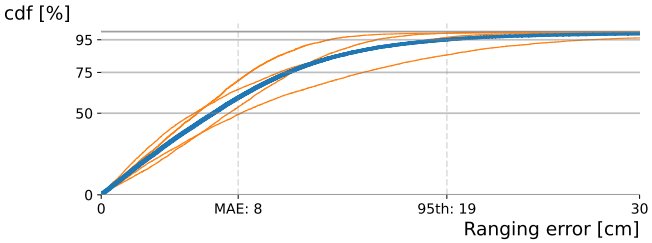

Fig. 5: Accuracy of TWR ranging errors. Over all four anchors (individual orange lines), the mean distance estimation (blue line) is accurate up to 8 cm while 95% of the errors are below 19 cm.

B. Angular accuracy

The angle, calculated with PDOA, at which the FINAL packet of the TWR exchange arrives is reported in the registers of the DW3000. In addition, we calculate this angle based on the recorded CIRs. The second part of the STS is received at a different antenna than the first part of this STS and as the preamble as well. The difference in phase from the CIRs can be used for estimating the angle. In Table I, the results of the three different methods (reported by the registers, based on CIR preamble and CIR STS2, and CIR STS1 and CIR STS2) are given. The reported angle in the registers is almost 2° less accurate as the results, calculated from the CIR information. The difference between taking the CIR of the preamble or the first part of the STS is only limited. In the next chapters, we will always calculate the angle based on the collected CIR information between STS1 and STS2.

	samples	PDoA DW3000	preamble STS2	STS1 STS2
Anchor 0	5858	8.2°	5.5°	6.4°
Anchor 1	5812	6.0°	3.4°	3.5°
Anchor 2	5732	6.5°	4.8°	4.8°
Anchor 3	5843	5.8°	3.7°	3.7°
All anchors	23245	6.6°	4.3°	4.6°

TABLE I: The errors of the three different methods to estimate the AoA for the four anchors show that calculating the angle based on the CIRs is more accurate than the reported values of the DW3000.

The field-of-view (FOV) of angular estimation refers to the range of angles within which the estimation demonstrates optimal accuracy and reliability. We conducted experiments with a slightly altered configuration, rotating the anchor nodes by 15 °such that larger angles can be measured in the setup. Using the same trajectory, we compared the angular estimation error against the true angle (Fig. 6). Our observations indicate a decline in performance as the incident angle increases. Notably, all three methods have their highest angular accuracy within a zone centered around 0°.

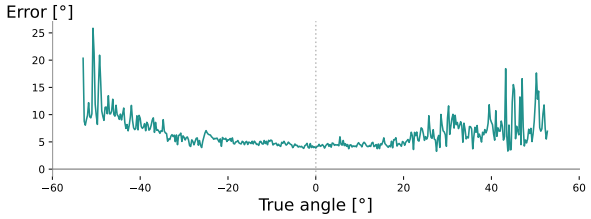

Fig. 6: The field of view over the measured angles: the angular accuracy deteriorates when the angle is larger than 45° in both directions.

C. Localization accuracy

In this section, we compare the localization accuracy of TWR, AoA, and combined. For TWR, we compare the system's accuracy with four, three, or two anchor nodes. Limiting the possible area where the tag can be and considering the anchors on the same side of this area, eliminates ambiguity between the two intersecting circles. However, positioning accuracy is low with two anchor nodes at the opposing side of the targeted area due to low dilution of precision (DOP) values and is not considered.

When all four anchor nodes are considered, TWR is the most accurate with an MAE of 18.7 cm over the 50 m^2 area. When adding angle information to the setup, the MAE decreases to 24.4 cm. The scenario where only angle information is utilized (MAE: 78.9 cm) is not advantageous in this setup. However, it can be considered in other scenarios: in systems with a large number of tags, it becomes feasible to localize a tag with a single UWB packet by simultaneously receiving at all anchors. If the number of anchors decreases, the accuracy of the system decreases due to the limited DOP. For TWR, the difference between 3 and 4 anchors is limited, but when only 2 anchors are used, the accuracy drops significantly. In systems that combine AoA and TWR, the performance also drops when fewer anchors are available with the system showing better robustness (lower 95th percentile and standard deviation) when a single anchor is used in comparison to a two anchor TWR approach. The combination of angle and distance information is therefore relevant for sparse and less demanding applications to increase robustness with fewer anchors. The results when using a LS approach are given in Table II.

D. Influence of post-processing

1) Influence of averaging on distance: The distance measurement in the data can be represented as the true distance between the tag and anchor superposed with an error factor. This error factor originates from propagation effects and measurement noise in the system. To mitigate this noise in the system, a moving average filter is tested that takes the average over the last n samples. The optimal value found for our dataset to average over is n equal to 6 or about 0.3 seconds. The average ranging error decreases with 0.6 cm while the individual anchor improvements range between 0 and 1.1 cm. This averaging factor of n will be used in further analysis.

Technique	#anchors	MAE [cm]	75th [cm]	95th [cm]	std [cm]
TWR	4	18.7	23.5	32.7	9.2
	3	21.4	26.7	39.1	16.3
	2	44.9	54.1	135.1	44.0
AoA	4	78.9	100.0	180.9	60.4
	3	94.1	116.0	224.1	96.5
	2	100.7	124.9	247.8	92.8
TWR + AoA	4	24.4	29.5	50.6	15.2
	3	29.9	36.4	72.3	21.3
	2	36.1	46.7	88.0	27.1
	1	48.4	64.5	118.8	40.8

TABLE II: Localization error for the different localization techniques with a LS positioning algorithm.

2) Influence of averaging on angle: The influence of averaging to reduce noise on the angle accuracy is investigated similarly. Averaging the last n samples reduces the noise but introduces latency and errors in dynamic environments. Our experimental dataset shows that taking a rolling window of the last 6 angles has the lowest angle error. We will consider this value when studying the localization that incorporates angles. The angle error over all four anchor nodes is now lowered to 3.9°. Therefore, the averaging denoises the measured angles significantly. Due to the dynamic movement of the data collection, averaging over more samples will influence the average angle accuracy due to latency effects.

3) Influence of averaging on localization: To improve the localization accuracy, the influence of averaging is investigated as it has been proven previously that using a moving average could improve the distance and angle error. In this experiment, we will apply a similar moving average filter to the ranges and angles before estimating the position and observing the influence on the localization error. This is compared to scenarios without a moving average filter and with a moving average filter applied to the positions. In Table III, the accuracy of the different tested scenarios is given. When applying filtering to the ranges and/or angles before injecting them into the localization algorithm, an increase of a few centimeters in performance can be noted. When applying an averaging filter to the position, the noise is filtered and the localization error decreases. When applying the filters both before and after the localization results in the best accuracy. A single anchor localization system is capable of localizing a target with a MAE of 43.3 cm. Adding an extra anchor can improve the localization to 32.4 cm. The incorporation of angle information in localization systems with 2 anchors is beneficial as it adds robustness and solves ambiguity problems.

4) Influence of Kalman filtering on localization: In the previous section, we discussed the localization results when incorporating ranging and angle information measured with the DW3000 UWB devices. As an alternative for the LS localization, a Kalman filter can be used to improve localization robustness. For every message exchange with an anchor, the Kalman filter updates its state: the position of the mobile tag and its velocity. For TWR, the Kalman filter uses the actual ranges as input, for AoA and hybrid localization, the Kalman filter uses direct positions. The influence of the Kalman filter for TWR localization is limited due to the already good performance in line-of-sight (LOS) situations. However, for AoA localization we see an improvement of the MAE between 6.4 and 9.7 cm. For the localization with both angle and distance information, using a Kalman filter improves the localization by about 2 cm. The performance with the Kalman filter is given in Table III.

Technique	#anchors	no [cm]	before [cm]	after [cm]	both [cm]	Kalman [cm]
TWR	4	18.7	15.5	17.7	14.9	18.7
	3	21.4	18.6	20.2	17.7	20.2
	2	44.9	43.1	40.6	39.3	363.3
AoA	4	78.9	63.3	70.0	61.7	71.8
	3	94.1	85.0	82.3	74.4	84.4
	2	100.7	85.8	95.7	84.3	94.3
TWR + AoA	4	24.4	17.6	20.9	16.6	22.7
	3	29.9	27.7	24.6	21.4	27.9
	2	36.1	33.8	32.8	32.4	34.5
	1	48.4	44.9	45.5	43.3	46.9

TABLE III: Use of averaging filter before and after LS localization.

VII. Discussions

In addition to demonstrating the possibility of single-anchor localization, this work also inspires further improvements. For example, more advanced filters could intelligently fuse angle and distance information from multiple anchors to derive the location. Such filter can take advanced quality metrics into account, e.g.: the total number of anchor nodes available, the link quality of each anchor node (giving less weight to NLOS links), the distance to each anchor (the inaccuracy of angle estimation increases when the distance increases), etc. Furthermore, similar to how CIR data is used for LOS/NLOS estimation, research could focus on how phase information can serve as an estimator of the link quality, to detect the pose and orientation of the tag and to detect NLOS conditions.

VIII. Conclusion

In this paper, we demonstrated the feasibility of single-anchor localization for use cases where deploying high anchor node densities is impossible. To this end, we analyzed the impact of combining TWR with AoA for different numbers of anchors, different AoA estimation techniques, and different postprocessing en filtering approaches. Our results show that TWR-only techniques remain more accurate when at least three anchors with good LOS are present, but that the combination of AoA with TWR is especially useful in use cases with two or fewer anchor nodes (due to costs, lack of cabling, etc.); or in harsh environmental conditions where only one or two anchor nodes have good LOS conditions. In such scenarios, single anchor node localization can obtain accuracies as low as 43.3 cm over a 50 m^2 at minimal deployment costs.

REFERENCES

[1] B. Van Herbruggen, B. Jooris, J. Rossey, M. Ridolfi, N. Macoir, Q. Van den Brande, S. Lemey, and E. De Poorter, "Wi-pos: A low-cost, open source ultra-wideband (uwb) hardware platform with long range sub-ghz backbone," *Sensors*, vol. 19, no. 7, p. 1548, 2019.

[2] M. Elsanhoury, P. Mäkelä, J. Koljonen, P. Välisuo, A. Shamsuzzoha, T. Mantere, M. Elmusrati, and H. Kuusniemi, "Precision positioning for smart logistics using ultra-wideband technology-based indoor navigation: A review," *IEEE Access*, vol. 10, pp. 44 413–44 445, 2022.

[3] B. Van Herbruggen, J. Vanhie-Van Gerwen, S. Luchie, Y. Durodié, B. Vanderborght, M. Aernouts, A. Munteanu, J. Fontaine, and E. De Poorter, "Selecting and combining uwb localization algorithms: insights and recommendations from a multi-metric benchmark," *IEEE Access*, 2024.

[4] D. Coppens, A. Shahid, S. Lemey, B. Van Herbruggen, C. Marshall, and E. De Poorter, "An overview of uwb standards and organizations (ieee 802.15. 4, fira, apple): Interoperability aspects and future research directions," *IEEE Access*, vol. 10, pp. 70 219–70 241, 2022.

[5] I. Dotlic, A. Connell, H. Ma, J. Clancy, and M. McLaughlin, "Angle of arrival estimation using decawave dw1000 integrated circuits," in *2017 14th Workshop on Positioning, Navigation and Communications (WPNC)*. IEEE, 2017, pp. 1–6.

[6] L. Botler, M. Gashi, K. Diwold, and K. Römer, "Machine learning-based models for phase-difference-of-arrival measurements using ultra-wideband transceivers," in *2022 21st ACM/IEEE International Conference on Information Processing in Sensor Networks (IPSN)*. IEEE, 2022, pp. 517–518.

[7] J. Tiemann, O. Fuhr, and C. Wietfeld, "Celidon: Supporting first responders through 3d aoa-based uwb ad-hoc localization," in *2020 16th International Conference on Wireless and Mobile Computing, Networking and Communications (WiMob)*. IEEE, 2020, pp. 20–25.

[8] M. Naseri, A. Shahid, G.-J. Gordebeke, S. Lemey, M. Boes, S. Van de Velde, and E. De Poorter, "Machine learning-based angle of arrival estimation for ultra-wide band radios," *IEEE Communications Letters*, vol. 26, no. 6, pp. 1273–1277, 2022.

[9] A. R. J. Ruiz and F. S. Granja, "Comparing ubisense, bespoon, and decawave uwb location systems: Indoor performance analysis," *IEEE Transactions on instrumentation and Measurement*, vol. 66, no. 8, pp. 2106–2117, 2017.

[10] S. Han, H. Yoo, H. Choo, and B.-J. Jang, "Ieee 802.15. 4z uwb angle of departure tag design for indoor positioning," in *2023 53rd European Microwave Conference (EuMC)*. IEEE, 2023, pp. 975–978.

[11] C. Gentner, T. Jost, W. Wang, S. Zhang, A. Dammann, and U.-C. Fiebig, "Multipath assisted positioning with simultaneous localization and mapping," *IEEE Transactions on Wireless Communications*, vol. 15, no. 9, pp. 6104–6117, 2016.

[12] B. Großwindhager, M. Rath, J. Kulmer, M. S. Bakr, C. A. Boano, K. Witrisal, and K. Römer, "Salma: Uwb-based single-anchor localization system using multipath assistance," in *Proceedings of the 16th ACM Conference on Embedded Networked Sensor Systems*, 2018, pp. 132–144.

[13] S. O. Schmidt, M. Cimdins, F. John, and H. Hellbrück, "Salos—a uwb single-anchor indoor localization system based on a statistical multipath propagation model," *Sensors*, vol. 24, no. 8, p. 2428, 2024.

[14] G. Mao, S. Drake, and B. D. Anderson, "Design of an extended kalman filter for uav localization," in *2007 Information, Decision and Control*. IEEE, 2007, pp. 224–229.